

PHOTOPRODUCTION OF ISOLATED PHOTONS, SINGLE HADRONS AND JETS AT NLO¹

Gudrun Heinrich

*II. Institut für theoretische Physik, Universität Hamburg,
Luruper Chaussee 149, 22761 Hamburg, Germany*

Abstract

The photoproduction of large- p_T charged hadrons and of prompt photons is discussed, for the inclusive case and with an associated jet, using predictions from the NLO partonic Monte Carlo program EPHOX. Comparisons to recent HERA data are also shown.

1 Introduction

At HERA, the photoproduction of jets has been measured with high statistics over the past years [1, 2, 3]. Data on and single charged hadron [4] and prompt photon [5, 6, 7] production are also available and have been compared to theoretical predictions [8]- [15], where in the prompt photon case the statistics is of course lower as the cross sections are small.

In photoproduction reactions, an almost real photon, emitted at small angle from the electron, interacts with a parton from the proton. The photon can either participate directly in the hard scattering ("direct photon") or act as a "resolved photon", in which case a parton stemming from the photon takes part in the hard interaction. Therefore photoproduction reactions offer a unique opportunity to constrain the parton distributions in the photon, especially the gluon distribution $g^\gamma(x)$. The latter is rather poorly constrained by LEP $\gamma^*\gamma$ data as it enters in this reaction only at next-to-leading order (NLO), whereas in ep photoproduction it enters already at leading order.

On the other hand, photoproduction reactions at HERA also could serve to constrain the gluon distribution in the *proton*. To determine the latter to a better accuracy is of particular interest in view of the LHC with its large gluon luminosity, $gg \rightarrow H$ being the dominant production mode for a light Higgs boson. As the photon represents a rather "clean" initial state, photoproduction reactions can be used to probe the proton in a way which is complementary to other experiments.

In what follows, the kinematic regions where gluon initiated subprocesses play a significant role will be identified and it will be argued that their relative contribution to the cross section can be enhanced by appropriate cuts, for the proton as well as for the photon case. For a more detailed study, the reader is referred to [16].

Comparisons to HERA data, especially to very recent (preliminary) H1 data on prompt photon plus jet production, will also be shown.

¹To appear in the proceedings of the Ringberg Workshop "New Trends in HERA Physics 2003", Ringberg Castle, Tegernsee, Germany, September 28 - October 3, 2003.

2 Theoretical aspects of charged hadron and prompt photon production

We will concentrate here on the two reactions $\gamma p \rightarrow h^\pm (+ \text{jet}) + X$ and $\gamma p \rightarrow \gamma (+ \text{jet}) + X$. Identifying a jet in addition to the prompt photon or hadron allows for a more detailed study of the underlying parton dynamics, and in particular for the definition of observables x_{obs}, x_{LL} which are suitable to study the parton distribution functions.

Comparing the reaction of charged hadron production versus prompt photon production, one is tempted to say that prompt photon production is more advantageous: Due to photon isolation, the dependence of the theoretical prediction on the non-perturbative fragmentation functions is negligible. Further, as will be shown in the following, the NLO prediction for the prompt photon cross section is not very sensitive to scale changes, which cannot be said for the $h^\pm (+ \text{jet})$ cross section [9]. On the other hand, the $\gamma + \text{jet}$ cross section is orders of magnitude smaller than the $h^\pm + \text{jet}$ cross section, and the identification of the prompt photon events among the huge background from the decay of neutral pions is experimentally not an easy task.

Photon isolation

Prompt photons can originate from two mechanisms: Either they stem directly from the hard interaction, or they are produced by the fragmentation of a hard parton. In order to distinguish them from the background stemming from the decay of light mesons, an *isolation criterion* has to be imposed: The amount of hadronic transverse energy E_T^{had} , deposited inside a cone with aperture R centered around the photon direction in the rapidity and azimuthal angle plane, must be smaller than some value E_T^{max} :

$$\begin{aligned} (\eta - \eta^\gamma)^2 + (\phi - \phi^\gamma)^2 &\leq R^2 \\ E_T^{\text{had}} &\leq E_T^{\text{max}}. \end{aligned} \quad (1)$$

For the numerical results we will follow the HERA conventions $E_T^{\text{max}} = 0.1 p_T^\gamma$ and $R = 1$.

Apart from reducing the background from secondary photons, isolation also substantially reduces the fragmentation component, such that the total cross section depends very little on the photon fragmentation functions.

Factorisation and scale dependence

The cross section for prompt photon production can be written symbolically as

$$d\sigma^{ep \rightarrow \gamma X}(P_e, P_p, P_\gamma) = \sum_{a,b} \int dx_e dx_p F_{a/e}(x_e, M) F_{b/p}(x_p, M) \{d\hat{\sigma}^{\text{dir}} + d\hat{\sigma}^{\text{frag}}\}$$

$$d\hat{\sigma}^{\text{dir}} = d\hat{\sigma}^{ab \rightarrow \gamma X}(x_a, x_b, P_\gamma, \mu, M, M_F)$$

$$d\hat{\sigma}^{\text{frag}} = \sum_c \int dz D_{\gamma/c}(z, M_F) d\hat{\sigma}^{ab \rightarrow c X}(x_a, x_b, P_\gamma/z, \mu, M, M_F).$$

In the case of the production of a single hadron, the partonic cross section $d\hat{\sigma}^{\text{dir}}$ is of course zero, and the fragmentation functions $D_{\gamma/c}(z, M_F)$ have to be replaced by the ones for hadrons, $D_{h/c}(z, M_F)$.

In photoproduction, $F_{a/e}(x_e, M)$ is a convolution

$$F_{a/e}(x_e, M) = \int dx^\gamma \int dy \delta(x^\gamma y - x_e) f_{\gamma/e}(y) F_{a/\gamma}(x^\gamma, M) \quad (2)$$

where the spectrum of quasi-real photons emitted from the electron is described by the Weizsäcker-Williams approximation

$$f_{\gamma/e}(y) = \frac{\alpha}{2\pi} \left\{ \frac{1 + (1-y)^2}{y} \text{Log} \frac{Q_{\text{max}}^2(1-y)}{m_e^2 y^2} - \frac{2(1-y)}{y} \right\}.$$

The function $F_{a/\gamma}(x^\gamma, M)$ in eq. (2) denotes the parton distribution function for a parton of type "a" in the resolved photon. In the case of a direct initial photon, one has $F_{a/\gamma}(x^\gamma, M) = \delta_{a\gamma} \delta(1 - x^\gamma)$. Therefore one can try to switch on/off the resolved photon by suppressing/enhancing large x^γ .

As the perturbative series in α_s for the partonic cross section is truncated, the theoretical prediction is scale dependent, depending on the renormalisation scale μ as well as on the initial/final state factorisation scales M/M_F . While the leading order cross section depends very strongly on the scales, the NLO cross section is already much more stable, as can be seen for example from Fig. 1 for the prompt photon inclusive cross section.

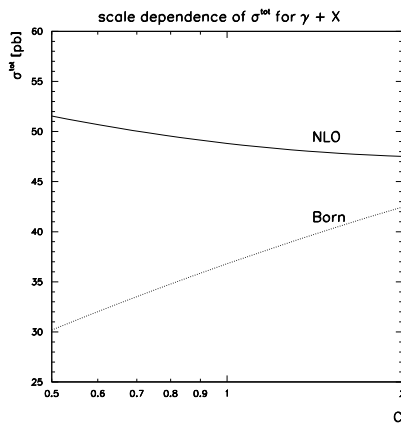


Figure 1: The scales have been set to $\mu = M = M_F = C p_T^\gamma$ with C varied between 0.5 and 2.

Observables x^γ, x^p

In order to reconstruct the longitudinal momentum fraction of the parton stemming from the proton respectively the photon from measured quantities, one can define the observables

$$\begin{aligned} x_{obs}^\gamma &= \frac{p_T e^{-\eta} + E_T^{jet} e^{-\eta^{jet}}}{2E^\gamma} \\ x_{obs}^p &= \frac{p_T e^\eta + E_T^{jet} e^{\eta^{jet}}}{2E^p} \end{aligned} \quad (3)$$

where p_T is the momentum of the prompt γ or the hadron, and η its (pseudo-)rapidity. However, as the measurement of E_T^{jet} can be a source of systematic errors at low E_T values, the following variable, which does not depend on E_T^{jet} , might be more convenient:

$$x_{LL}^{p,\gamma} = \frac{p_T (e^{\pm\eta} + e^{\pm\eta^{jet}})}{2E^{p,\gamma}} \quad (4)$$

The variable x_{LL}^γ also has the advantage that it has a smoother behaviour for $x^\gamma \rightarrow 1$.

3 Numerical studies

Unless stated otherwise, the following input for the numerical results is used: The center of mass energy is $\sqrt{s} = 318 \text{ GeV}$ with $E_e = 27.5 \text{ GeV}$ and $E_p = 920 \text{ GeV}$. The maximal photon virtuality is $Q_{\text{max}}^2 = 1 \text{ GeV}^2$, and $0.2 < y < 0.7$. For the parton distributions in the proton we take the MRST01 [17] parametrisation, for the photon we use AFG04 [18] distribution functions and BFG [19] fragmentation functions. For the charged hadron fragmentation functions we use BFGW [23] as default. We take $n_f = 4$ flavours, and for $\alpha_s(\mu)$ we use an exact solution of the two-loop renormalisation group equation, and not an expansion in $\log(\mu/\Lambda)$. The default scale choice is $M = M_F = \mu = p_T$. Jets are defined using the k_T -algorithm.

3.1 The NLO program EPHOX

All numerical results shown here are obtained by the NLO partonic Monte Carlo program EPHOX [20], which allows to obtain integrated cross sections as well as fully differential distributions for the reactions considered here. The program contains the full NLO corrections to all four categories of subprocesses direct-direct, direct-fragmentation, resolved-direct and resolved-fragmentation. It also contains the quark loop box diagram $\gamma g \rightarrow \gamma g$ with a flag to turn it on or off. EPHOX can be obtained at <http://wwwlapp.in2p3.fr/laphth/PHOX.FAMILY/main.html>, together with a comfortable user interface and detailed documentation.

3.2 The gluon distribution in the photon

In order to constrain the gluon distribution $g^\gamma(x^\gamma)$ in the photon, one has to focus on a kinematic region where the gluon content of the resolved photon is large, i.e. on small values of x^γ . According to eqs.(3) and (4), small x^γ corresponds to large values of η and η^{jet} , which means that the forward rapidity region is particularly interesting. Fig. 2 illustrates for the prompt photon plus jet cross section that the gluon distribution $g^\gamma(x^\gamma)$ only becomes important in the very forward region $\eta^\gamma \gtrsim 1.5$ if the rapidity of the jet is integrated over the range $-1 < \eta^{jet} < 2.3$. However, the relative importance of the gluon distribution $g^\gamma(x)$ can be enhanced by restricting both rapidities, the one of the photon *and* the one of the jet, to the forward region. Fig. 3a shows that with the cuts $\eta^\gamma, \eta^{jet} > 0$, the resolved photon component makes up for a major part of the cross section, but mainly consists of quarks, while for $\eta^\gamma > 0.5, \eta^{jet} > 1.5$, the gluon in the photon contributes about 40% to the total cross section, as shown in Fig. 3b.

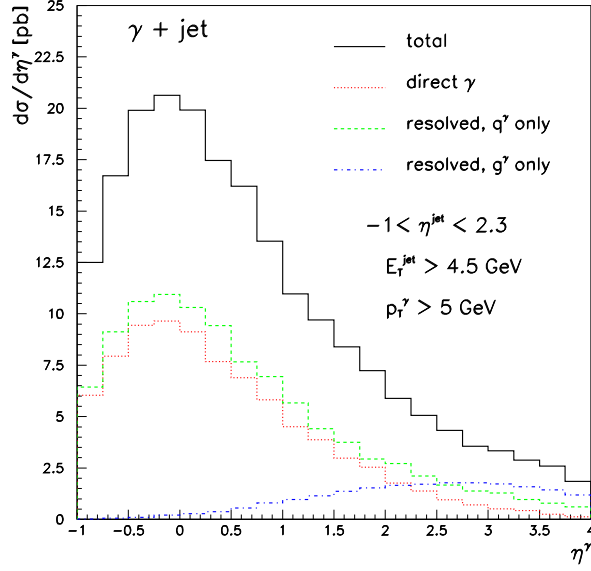


Figure 2: Rapidity range where the gluon in the photon becomes important

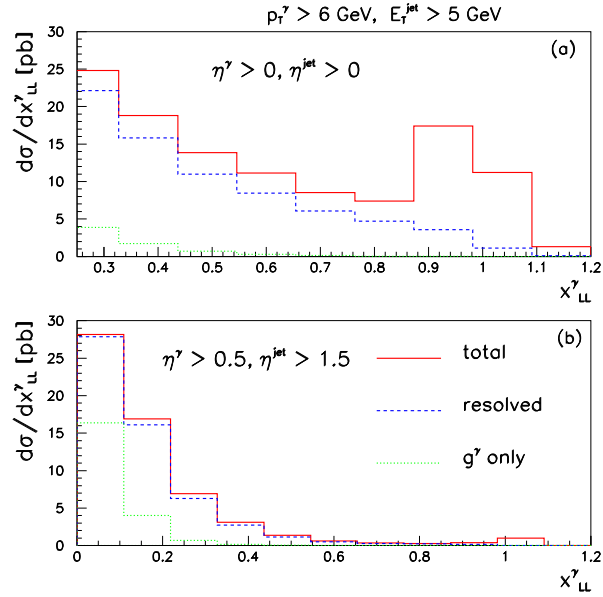


Figure 3: The rapidity cuts $\eta^\gamma > 0.5, \eta^{jet} > 1.5$ substantially enhance the relative contribution of the gluon in the resolved photon

3.3 The gluon distribution in the proton

The gluon distribution in the proton is large for small x^p , corresponding to small rapidities. From Fig. 4 one can indeed see that the relative contribution of subprocesses initiated by a gluon from the proton to the $h^\pm + \text{jet}$ cross section is about 73% if both rapidities are restricted to the backward region, $-2 < \eta, \eta^{jet} < 0.5$. The analogous is *not* true for the prompt photon + jet cross section, where the gluon contribution makes up only 13% of the total cross section if the rapidities are restricted to the range $-2 < \eta^\gamma, \eta^{jet} < 0$. This is due to the fact that at small x^p values, x^γ is large, such that direct initial photons should dominate. However, the subprocess

$g^p + \gamma \rightarrow \gamma(\text{direct}) + \text{jet}$ does not exist at leading order, and the subprocess $g^p + \gamma \rightarrow q + \text{jet}$, where the quark subsequently fragments into a photon, is suppressed by isolation. Therefore, in the case of the $\gamma + \text{jet}$ cross section, the

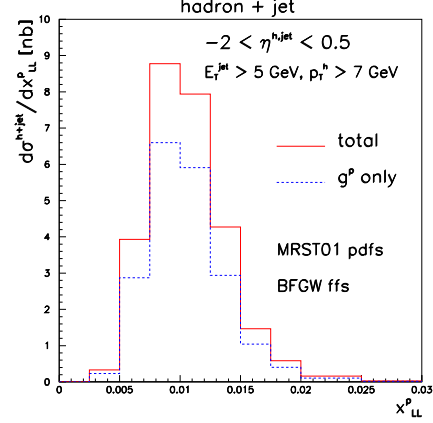


Figure 4: The gluon (from the proton) contribution to the $h^\pm + \text{jet}$ cross section at small rapidities.

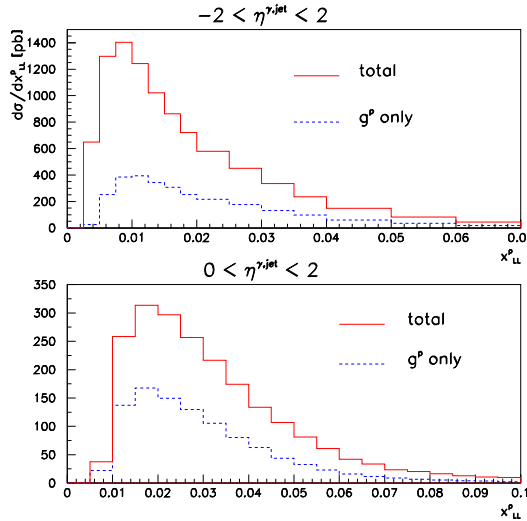


Figure 5: The relative contribution of gluon initiated processes to the $\gamma + \text{jet}$ cross section can be enhanced by the rapidity cuts $0 < \eta^\gamma, \eta^{jet} < 2$. The p_T cuts are $E_T^{jet} > 5 \text{ GeV}$, $p_T^\gamma > 6 \text{ GeV}$.

subprocess $g^p + \gamma \rightarrow \gamma + q$ is the dominant one involving g^p whereas in the case of the hadron+jet cross section, $g^p + \gamma \rightarrow q + \bar{q}$ is dominant at small x^p . The virtue of this behaviour of the prompt photon cross section is that the region

where g^p initiated subprocesses are important is *not* restricted to negative rapidities. As can be seen from Fig. 5, the rapidity cuts $0 < \eta^{\gamma, jet} < 2$ enhance the relative contribution of the gluon g^p to the $\gamma + \text{jet}$ cross section, because they select a region where $g^p + q^\gamma$ initiated subprocesses are important. Note that this rapidity domain is more accessible experimentally than the very backward region.

4 Comparison to HERA data

4.1 Charged hadrons

For the case of single charged hadron production, only data for $h^\pm + X$, but not for $h^\pm + \text{jet} + X$ are available so far [4]. The analysis uses a minimum p_T of 3 GeV for the hadron, which is rather close to the non-perturbative regime. This induces a large theoretical uncertainty due to differences in the parametrisation of the fragmentation functions [21, 22, 23] at low p_T (see Fig. 6), and also a large scale dependence. If a minimum p_T of 7 GeV is chosen for the hadron, the cross section is reduced, but the theoretical uncertainty is much smaller [9].

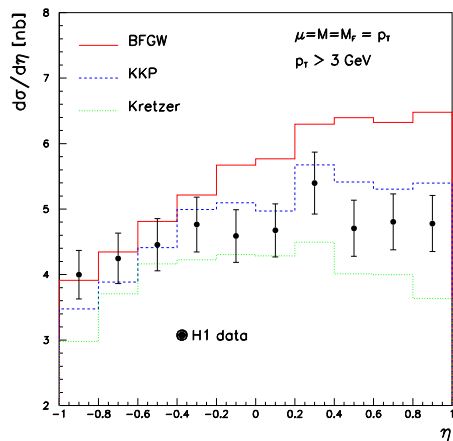


Figure 6: Predictions obtained with different fragmentation functions compared to H1 data.

4.2 Prompt photons (inclusive)

For inclusive prompt photon production, ZEUS data [5, 6] as well as preliminary H1 data [7] are available². In Fig. 7, one observes that the ZEUS data are above the NLO prediction in the backward region. At large rapidities, there is a trend that theory is above both H1 and ZEUS data. As already mentioned in the introduction, this effect is very likely due to photon isolation: A sizeable amount of hadronic transverse energy in the isolation cone may stem from the underlying event. Therefore, even

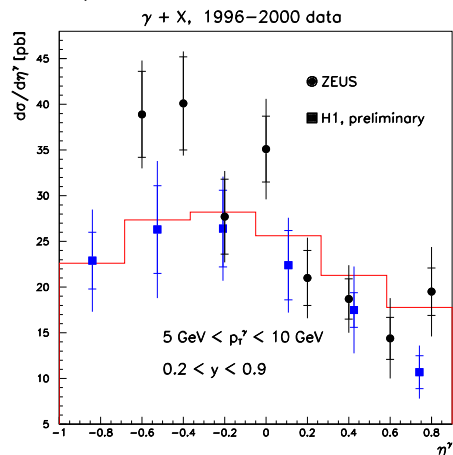


Figure 7: Comparison of inclusive prompt photon data with the NLO QCD prediction.

²In order to be able compare to the ZEUS data taken at $E_p = 820$ GeV and $0.2 < y < 0.9$, the H1 data taken at $E_p = 920$ GeV and $0.2 < y < 0.7$ have been corrected using PYTHIA [7].

direct photon events may be rejected, leading to a decrease of the cross section. This fact cannot be simulated by a partonic Monte Carlo, such that the NLO predictions tend to be above the data in kinematic regions where the underlying event activity is expected to be large.

4.3 Prompt photon + jet

In the rapidity distribution for the γ + jet cross section, the effect mentioned above is again visible at large rapidities. To estimate its impact, H1 recently made an analysis [7, 24] where the NLO result is corrected for multiple interaction effects. As can be seen from Fig. 8, the corrections are indeed most pronounced in the forward region where the underlying event activity from the resolved photon remnants is expected to be larger, and they improve the agreement between data and theory. Fig. 8 also shows that the γ +jet cross section is very stable with respect to scale variations.

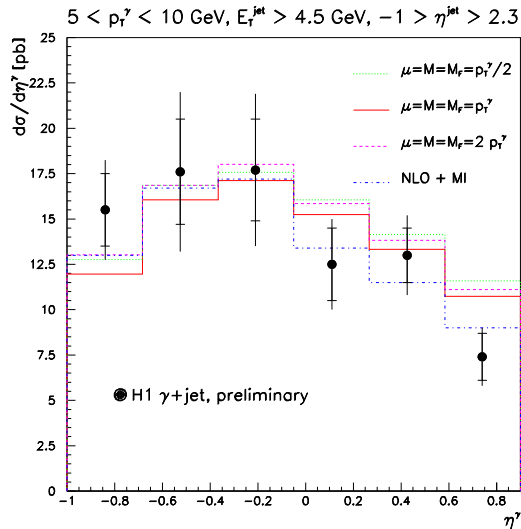


Figure 8: Comparison of preliminary H1 data to the NLO prediction with different scale choices. NLO+MI denotes the result where the partonic prediction has been corrected for multiple interaction effects.

4.4 Study of intrinsic $\langle k_T \rangle$

The ZEUS collaboration made an analysis on prompt photon + jet data to study the "intrinsic" parton transverse momentum $\langle k_T \rangle$ in the proton [6]. To this aim, the $\langle k_T \rangle$ -sensitive observables p_\perp , the photon momentum component perpendicular to the jet direction, and $\Delta\phi$, the azimuthal acollinearity between photon and jet, have been studied. To suppress contributions to $\langle k_T \rangle$ from the resolved photon, the cut $x_\gamma^{obs} > 0.9$ has been imposed. To minimise calibration uncertainties, only normalized cross sections have been considered, as an additional $\langle k_T \rangle$ mainly changes the *shape* rather than the absolute value of the cross section. The best fit with PYTHIA 6.129 lead to the result $\langle k_T \rangle = 1.69 \pm 0.18(\text{stat})_{-0.20}^{+0.18}(\text{sys})$ GeV, which includes the shower contribution to $\langle k_T \rangle$. On the other hand, the NLO program EPHOX is able to describe the data without including an additional $\langle k_T \rangle$. This is shown in Fig. 9, where also the minimum E_T^{jet} has been varied in order to estimate the impact of an uncertainty in the determination of the jet energy and of choosing symmetric cuts ($p_T^\gamma > 5$ GeV has been used in the experimental analysis).

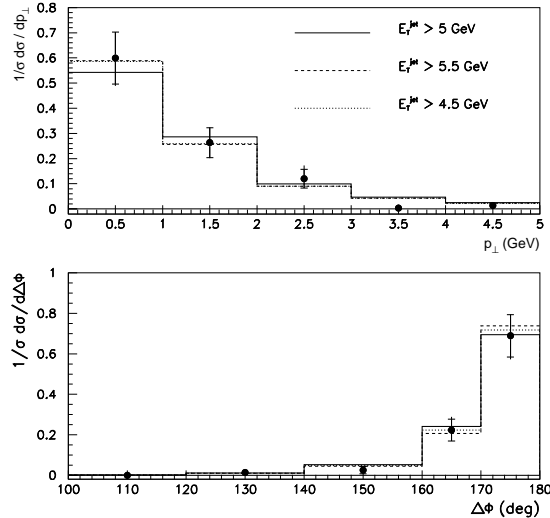


Figure 9: ZEUS data for the normalised cross sections differential in p_{\perp} and $\Delta\phi$ compared to the EPHOX prediction for different cuts on the minimum jet transverse energies.

5 Conclusions

The reactions $\gamma p \rightarrow \gamma + \text{jet} + X$ and $\gamma p \rightarrow h^{\pm} + \text{jet} + X$ offer the possibility to constrain the gluon density in the photon and in the proton. It has been shown that appropriate rapidity cuts can enhance the relative contribution of gluon initiated processes.

Comparing the predictions of the partonic Monte Carlo NLO program EPHOX to HERA data, the following observations can be made: For inclusive single charged hadron production, the H1 data are well described, but the theoretical uncertainties from fragmentation functions and scale variations are large. These large uncertainties can mainly be attributed to the fact that a minimal p_T of 3 GeV for the hadron is too close to the non-perturbative regime. A p_T^{min} of 7 GeV improves the stability of the theoretical predictions.

The rapidity distributions for inclusive prompt photon production as well as for $\gamma + \text{jet}$ show an interesting feature: At large rapidities, the NLO prediction always tends to overshoot the data. It has been argued that this behaviour might be attributed to photon isolation: Due to hadronic activity stemming from the underlying event in the isolation cone, even direct photons in the final state may be rejected by the isolation cut, thus leading to a lower cross section than the (partonic) Monte Carlo prediction, especially in the forward region where the probability of resolved photon remnants is higher. A recent H1 analysis which corrects the NLO prediction bin per bin for multiple interaction effects corroborates this explanation.

Finally, the predictions of EPHOX have been compared to a ZEUS analysis on prompt photon+jet data where the intrinsic $\langle k_T \rangle$ of the proton is studied,

and it has been found that the NLO prediction describes the data very well without introducing an extra $\langle k_T \rangle$.

Acknowledgements

I would like to thank the organisers of the Ringberg workshop for an interesting and pleasant meeting, and J. Gayler, R. Lemrani and P. Bussey for discussions on the data. I also wish to thank my collaborators M. Fontannaz and J. Ph. Guillet.

References

- [1] C. Adloff *et al.* [H1 Collaboration], DESY-02-225, hep-ex/0302034.
- [2] S. Chekanov *et al.* [ZEUS Collaboration], Phys. Lett. B **560** (2003) 7 [hep-ex/0212064].
- [3] J. Cvach, *in these proceedings*.
- [4] C. Adloff *et al.* [H1 Collaboration], Eur. Phys. J. C **10** (1999) 363 [hep-ex/9810020].
- [5] J. Breitweg *et al.* [ZEUS Collaboration], Phys. Lett. B **472** (2000) 175 [hep-ex/9910045];
J. Breitweg *et al.* [ZEUS Collaboration], Phys. Lett. B **413** (1997) 201 [hep-ex/9708038].
- [6] S. Chekanov *et al.* [ZEUS Collaboration], Phys. Lett. B **511** (2001) 19 [hep-ex/0104001].
- [7] H1 Collaboration, submitted to the Int. Europhysics Conference on High Energy Physics, EPS03, July 2003, Aachen (Abstract 093), and to the XXI Int. Symposium on Lepton and Photon Interactions, LP03, August 2003, Fermilab.
- [8] B. A. Kniehl, G. Kramer and B. Pötter, Nucl. Phys. B **597** (2001) 337 [hep-ph/0011155].
- [9] M. Fontannaz, J. P. Guillet and G. Heinrich, Eur. Phys. J. C **26** (2002) 209 [hep-ph/0206202].
- [10] L. E. Gordon and W. Vogelsang, Phys. Rev. D **52**, 58 (1995).
- [11] L. E. Gordon, Phys. Rev. D **57** (1998) 235 [hep-ph/9707464].
- [12] M. Fontannaz, J. P. Guillet and G. Heinrich, Eur. Phys. J. C **21** (2001) 303 [hep-ph/0105121].
- [13] M. Fontannaz, J. P. Guillet and G. Heinrich, Eur. Phys. J. C **22** (2001) 303 [hep-ph/0107262].
- [14] M. Krawczyk and A. Zembrzuski, Phys. Rev. D **64** (2001) 114017 [hep-ph/0105166].

- [15] A. Zembrzuski and M. Krawczyk, hep-ph/0309308.
- [16] M. Fontannaz, G. Heinrich, hep-ph/0312009.
- [17] A. D. Martin, R. G. Roberts, W. J. Stirling and R. S. Thorne, Eur. Phys. J. C **23** (2002) 73.
- [18] P. Aurenche, J. P. Guillet and M. Fontannaz, Z. Phys. C **64** (1994) 621;
P. Aurenche, J. P. Guillet and M. Fontannaz, new version of AFG, publication in preparation.
- [19] L. Bourhis, M. Fontannaz and J. Ph. Guillet, Eur. Phys. J. C **2**, 529 (1998).
- [20] For a detailed description of EPHOX, see ref. [12] and <http://www1app.in2p3.fr/lapth/PHOX.FAMILY/main.html>.
EPHOX is actually part of a larger family of NLO Monte Carlo programs, containing also programs for hadron-hadron collisions and e^+e^- photoproduction.
- [21] S. Kretzer, Phys. Rev. D **62** (2000) 054001 [hep-ph/0003177].
- [22] B. A. Kniehl, G. Kramer and B. Potter, Nucl. Phys. B **582** (2000) 514 [hep-ph/0010289].
- [23] L. Bourhis, M. Fontannaz, J. P. Guillet and M. Werlen, Eur. Phys. J. C **19** (2001) 89 [hep-ph/0009101].
- [24] R. Lemrani [H1 Collaboration], *Talk given at the 11th International Workshop on Deep Inelastic Scattering (DIS 2003), St. Petersburg, Russia, April 2003*, hep-ex/0308066;
R. Lemrani-Alaoui, “*Prompt photon production at HERA*”, Ph.D. thesis, DESY-THESIS-2003-010, available at http://www-h1.desy.de/publications/theses_list.html.